Sub-10 cm^3 Interferometric Accelerometer With Nano-g Resolution

Nin C. Loh, Martin A. Schmidt, *Senior Member, IEEE*, and Scott R. Manalis

***Abstract*—A high-resolution accelerometer with a bulk-micromachined silicon proof mass and an interferometric position sensor was developed for measuring vibratory accelerations. The interferometer consists of interdigitated fingers that are alternately attached to the proof mass and support substrate. Illuminating the fingers with coherent light generates a series of diffracted beams. The intensity of a given beam depends on the out-of-plane separation between the proof mass fingers and support fingers. Proof masses with mechanical resonances ranging from 80 Hz to 1 kHz were fabricated with a two mask process involving two deep reactive ion etches, an oxide etch stop, and a polyimide protective layer. The structures were packaged with a laser diode and photodiode into 8.6-cm^3 acrylic housings. The 80-Hz resonant proof mass has a noise equivalent acceleration of 40 ng/rt Hz and a dynamic range of 85 dB at 40 Hz. [730]**

I. Introduction

ACCELEROMETERS that resolve accelerations in the nano-g range are necessary for measuring seismic disturbances as well as gravitational waves [1], [2]. The key components for a nano-g accelerometer are a low resonant frequency proof mass and a displacement sensor with sub-angstrom resolution. Over the last decade, a major effort in microfabricating nano-g accelerometers has used electron tunneling as the position detector of a bulk-micromachined proof mass [3]–[5]. Most high-resolution tunneling accelerometers consist of a large proof mass (10 to 40 mg) with a conductive side that is brought within 10 angstroms of the reference tunneling tip. This strict tolerance increases the likelihood of the proof mass crashing into the tip during large accelerations. For this reason, tunneling accelerometers typically operate in force-feedback where the tunneling current is used to control a deflection voltage that keeps the proof mass stationary. Recently, researchers have microfabricated accelerometers based on electron tunneling transducers that resolve 30 ng/rt Hz between 7 Hz and 1.1 kHz [6] with a closed-loop dynamic range of over 90 dB.

Manuscript received July 24, 2001; revised November 14, 2001. This work was supported by the MIT Media Laboratory's Things That Think (TTT) Consortium. Subject Editor G. B. Hocker.

N. C. Loh was with the Media Laboratory, Massachusetts Institute of Technology, Cambridge, MA 02139 USA. He is now with Zyomyx, Inc., Hayward, CA 94545 USA.

M. A. Schmidt is with Microsystems Technology Laboratories, Department of Electrical Engineering and Computer Science, Massachusetts Institute of Technology, Cambridge, MA 02139 USA.

S. R. Manalis is with the Media Laboratory, MIT, 20 Ames St. E15-422, Cambridge, MA 02139 USA (e-mail: scottm@media.mit.edu).

Publisher Item Identifier S 1057-7157(02)04977-6.

Optical interference transducers are capable of achieving a position resolution equivalent to electron tunneling transducers. Interferometric displacement sensors can take many forms, including a Michelson interferometer [7] or a Fabry–Pérot cavity [1]. More recently, an interferometer with simple alignment procedure was developed to measure the deflection of atomic force microscope cantilevers [8]–[10]. This interferometer measures the intensity of a single mode diffracted off an array of fingers that are alternately attached to the cantilever tip and support substrate. The intensity of the diffracted modes depends on the out-of-plane offset between the two sets of fingers and is given by

$$I(d) = I_o \sin^2\left(\frac{2\pi d}{\lambda}\right) \tag{1}$$

where d is the offset and λ is the illumination wavelength [8]. Using this interferometer, the deflection of the cantilever can be resolved to 3×10^{-3} Å at 10 Hz [8]. Moreover, when the initial offset is set near the most linear regions (1), or the points of inflection, the output is linear within a 5% error up to a tenth of the wavelength of the light source, or 600 Å of motion for red light [11]. Due to this linearity, an accelerometer based on such a position transducer could achieve a dynamic range of 100 dB without the use of any force-feedback.

The interferometric accelerometer consists of a suspended bulk-micromachined proof mass with protruding fingers that are interleaved with fingers extending from the support substrate as shown in Fig. 1. When the fingers are illuminated with coherent light, a diffraction pattern is reflected. The movement of the proof mass, and hence its acceleration, is determined by measuring the intensity of one of the diffracted beams. The sensitivity and linearity of our accelerometer depend on the initial offset, or bias, of the proof mass. Since the device does not use force-feedback, this bias is determined by gravity (which we can control, to a certain extent, with the sensor tilt) and the residual stress of the silicon support beams.

The first accelerometer to use interdigitated fingers as a position detector resolved micro-g vibrations [12]. However, the fabrication had low reproducibility and yield ($<$10%), and was not suitable for low resonant frequency proof masses. Furthermore, the device was not packaged and its ultimate limit of resolution had not been measured. In this paper, we present a reliable process for fabricating proof masses with resonant frequencies as low as 80 Hz. We have also packaged the open-loop interferometric accelerometer into a small volume and characterized its sensitivity, noise, and linearity for vibratory excitations.

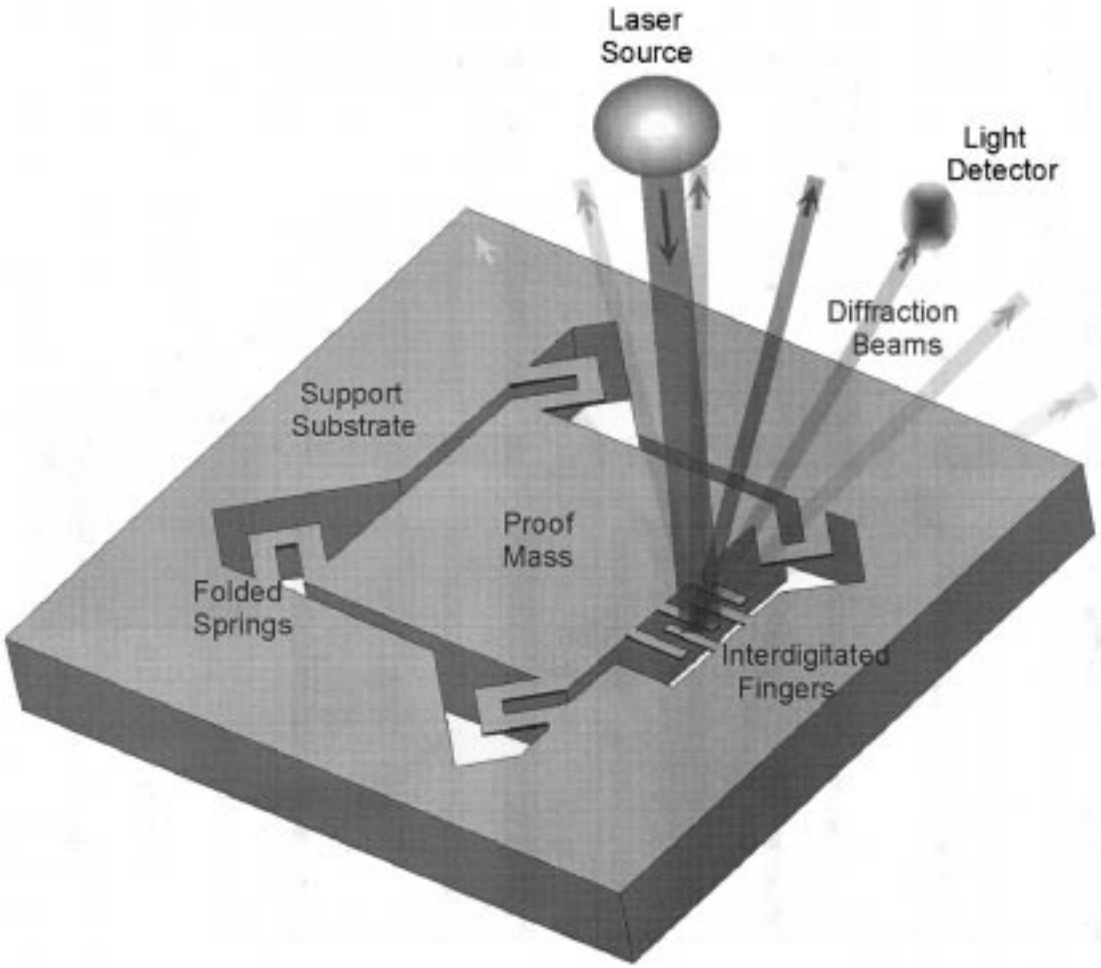

Fig. 1. Drawing of folded-pinwheel interferometric accelerometer. The intensity of a diffraction mode reflected off the interdigitated fingers is used to determine the displacement of the proof mass normal to the plane of die.

II. Design and Fabrication

The original interferometric accelerometer proof mass was suspend from a rectangular cantilever [12]. We choose to suspend the proof mass with the diagonal, "folded pinwheel" springs in Fig. 1 because it is more linear for motion normal to the plane of the device. Linearity of motion is important because we want to operate the accelerometer in open-loop without the use of linearization circuitry. Furthermore, the second and third resonant modes, composed of rotations about the diagonal of the proof mass, occur at a factor of $\sqrt{3}$ above the first resonant mode [13]. Moreover, the symmetry of the pinwheel springs allow the mass to rotate slightly making it less sensitive to external strains. Lastly, folded springs allow the fabrication of long, highly compliant springs without significantly increasing the size of the die.

The first interferometric accelerometer proof mass was fabricated with a two mask, CMOS compatible process that had low reproducibility and yield. It consisted of two timed deep reactive ion etches (DRIEs) in a plain silicon wafer and an acetone release. We used the same process with two improvements. First, a buried oxide layer in the substrate was used to provide a consistent etch stop for the DRIE, which is 100 times more selective for silicon than for oxide. This eliminates the dependence of the final spring thickness to variations in etch rate across the wafer and on different wafers. The second improvement was a polyimide film to serve as a support for the delicate springs and fingers during the long DRIE etch that defines the proof mass. The low pressure in the DRIE chamber can create a destructive pressure differential across the thin springs. The polyimide also allows the structures to be released dry, without the breakage and stiction problems accompanying the previous acetone release.

The proof mass wafer process started with a 100 mm, double-side polished silicon-on-insulator (SOI) wafer with a 20-μm device layer, a 1-μm-buried oxide layer, and a 381.5 -μm-Si handle layer. The springs and fingers are defined by the thin device layer, and the proof mass is composed of all three layers. First, 0.5 μm of thermal oxide was grown [see Fig. 2(a)] and patterned with 1 μm of resist (Olin OCG825) and plasma etched on the device layer side. Next the exposed device layer silicon was deep reactive ion etched all the way to the buried oxide layer as shown in Fig. 2(b). After stripping the resist, we spun cast 20 μm of polyimide (Hitachi PI2611) on the device layer side [see Fig. 2(c)] and cured at 350 °C for 30 min. We then patterned the backside of the wafer with 10 μm of resist (Hoechst–Celanese AZ4620), removed the exposed oxide in buffered oxide etchant (BOE), and deep reactive ion etched the exposed handle layer to the buried oxide layer as shown in Fig. 2(d). We then removed the backside thermal oxide and the exposed buried oxide in BOE as shown in Fig. 2(e). Finally, we

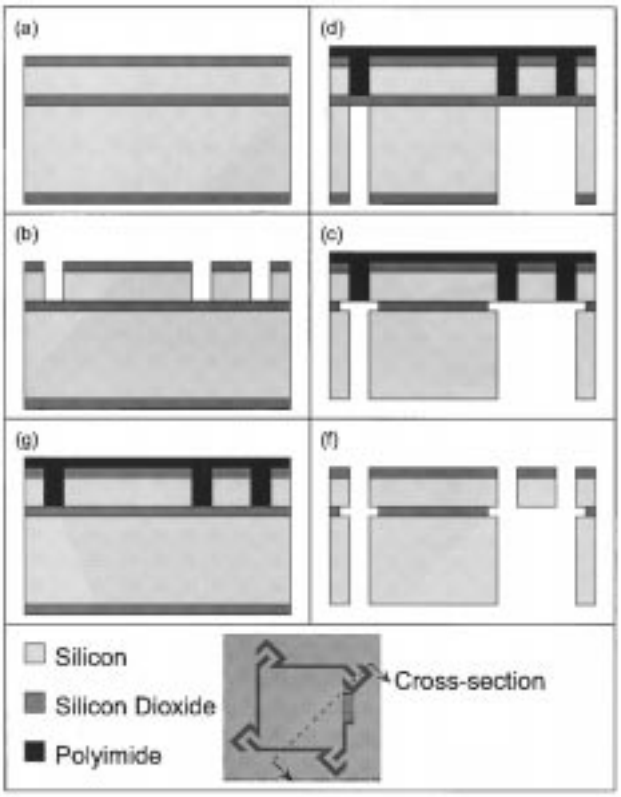

Fig. 2. Fabrication process for interferometric accelerometer. (a) Thermal oxidation of SOI wafer. (b) Topside lithography and DRIE etch to define fingers, springs, and mass. (c) Spin-on and cure polyimide. (d) Bottomside lithography and DRIE etch to define mass. (e) BOE etch of box oxide. (f) Ash polyimide in oxygen plasma.

etched away the polyimide in an oxygen plasma [see Fig. 2(f)]. This last step releases the proof mass and allows the dies to be removed by only breaking several thin tabs.

Using this process, we released proof masses with resonant frequencies ranging from 80 Hz to 1 kHz with 100% yield. The length of the folded-pinwheel springs were obtained by entering a sensible proof mass size (30 mg, 5.6 mm $\times$ 5.6 mm) and spring width (140 μm) into ProEngineer and an analytical model in which the springs run parallel to the mass [13]. The simulation and model agree to better than 5% up to about 1 kHz resonant frequency. Near this resonant frequency, the length of each spring becomes comparable to its width, and the error between the effective spring length of the model and the actual spring length in the diagonal pinwheel becomes significant.

In the center of one side of the proof mass are fifty 175 μm $\times$ 6 μm $\times$ 20 μm interdigitated fingers separated by gaps of 3 μm. The fingers are twice as wide and half as long as the ones on the original interferometric accelerometer to eliminate breakage and stiction. The fingers on the proof mass overlap with the fingers on the support substrate for 125 μm, giving an area of 450 μm $\times$ 125 μm in which to focus the laser. Fig. 3 is a micrograph of the interdigitated fingers showing successful release.

III. Packaging

The accelerometer package consists of four acrylic pieces cut with a CO_2 laser. The bottom piece holds the proof mass die and has a hole under the proof mass to allow it to oscillate. The top piece holds a silicon die with a 200-μm $\times$ 150-μm p–n junction diode wirebonded to an alumina plate. Coaxial cables carrying the output signal are soldered to this plate. Attached to the side of the top piece is a 670 nm, 5 mW, laser diode with a lens attached to the window that focuses the light onto the fingers. The two middle pieces form a 6.7 mm shim to allow the diffraction modes to spread and be differentiated from each other. The spacing x of the modes at a distance h from the interdigitated fingers of pitch d is $x = h\lambda/2d$ where λ is the wavelength of the light. The separation of 6.7 mm and pitch of 9 μm correspond to a mode spacing of 250 μm. We measured the first mode because lower order modes are less affected by wavelength and phase noise [10] and the specular (0th) mode includes undesirable reflections off the bulk. The package is 2.33 cm $\times$ 2.20 cm $\times$ 1.67 cm (8.6 cm^3) and weighs 9 g. It has five necessary leads: three for the laser diode and two for the photodiode.

IV. Results

We packaged interferometric accelerometers with resonant frequencies of 80 Hz, 430 Hz, and 1 kHz and tested them on a piezoelectric shaker mechanically isolated on a floated optics table. On the shaker plate we mounted our package and a reference accelerometer (Analog Devices ADXL105JQC) with their sensitive axes in the horizontal direction of actuation. Mounted beside the actuation stage was a low noise seismic accelerometer (Wilcoxon 731) used to measure background seismic vibrations. We used a constant power driver to drive the laser diode and a current amplifier to amplify the current from the photodiode.

We measured the sensitivity of the packaged interferometric accelerometers using a LabVIEW program (National Instruments) which controlled the function generator that drove the shaker. At each frequency, the stage is driven at two different accelerations, and a DSP lock-in amplifier extracts the component of both the test and reference accelerometer signals at that frequency. Because the frequency of the test accelerometer output matched the input frequency and phase, we were assured that the static offset of the fingers was biased at a point of positive sensitivity away from the extrema of (1). (The output frequency becomes twice the input frequency when the displacement crosses the extrema.) The sensitivity was calculated by taking the ratio of the change in sensor signal to the change in acceleration. We found that the sensitivity of the accelerometers scale with the inverse square of the resonant frequency, which means that the intensity of the modes in each package is of equal magnitude. This suggests that the packaging is highly reproducible. Fig. 4 shows the sensitivity of the 80 Hz resonant frequency sensor which fits a second-order transfer function with a Q of 68. We also tested the sensitivity of the proof mass to accelerations in two directions tangent to its plane. The sensitivity of the sensor to accelerations directed along and across the fingers was found to be at least 250 and 50, respectively, times less than the sensitivity to accelerations normal to the plane. Because we did not use another reference accelerometer to ensure that the test sensor was not being accelerated in its sensitive axis, the actual cross-axis sensitivity may actually be lower than our result.

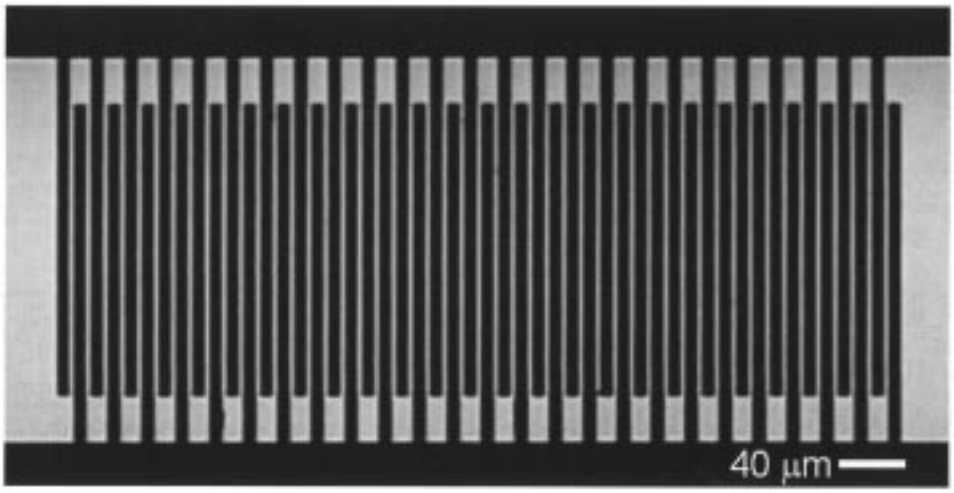

Fig. 3. Optical micrograph (transmitted illumination) showing the released interdigitated fingers.

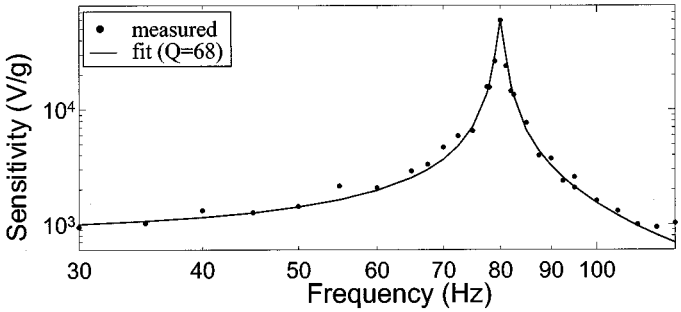

Fig. 4. Sensitivity of 80 Hz packaged interdigital accelerometer.

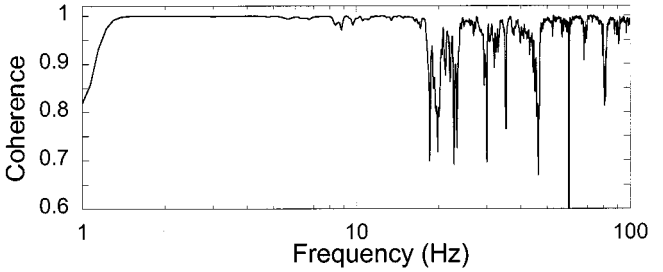

Fig. 5. Coherence between two packaged interdigital accelerometers with a resonant frequency of 80 Hz.

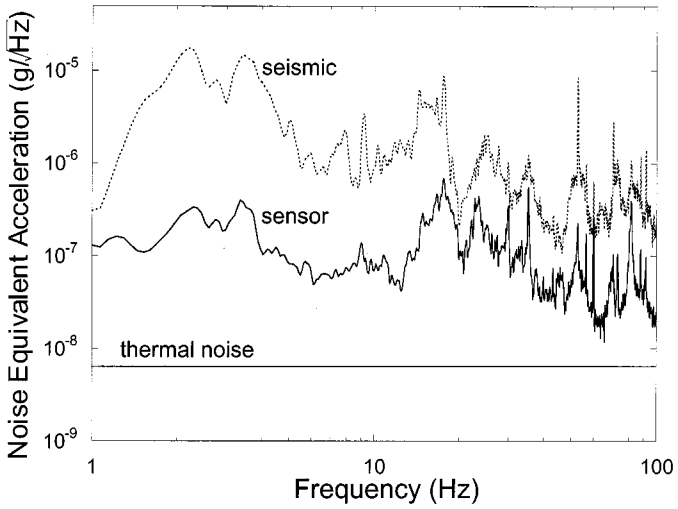

Fig. 6. Noise equivalent acceleration from the power spectrum density of an 80 Hz resonant accelerometer. "seismic" is the NEA from a mechanical isolated accelerometer, "sensor" is the NEA scaled by the coherence between two 80 Hz resonant accelerometers and "thermal" noise is a plot of (2).

The resolution of an accelerometer is ultimately limited by thermal noise of the proof mass

$$a_{TM} = \sqrt{\frac{8\pi k_B T f_o}{mQ}} = 3.21 \times 10^{-10}\ \mathrm{J}^{1/2}\sqrt{\frac{f_o}{mQ}} \qquad (2)$$

where T is temperature, k_B is Boltzman's constant, m is the mass, f_o is the resonant frequency, and Q is the quality factor [14]. For the device characterized in Fig. 4, $f_o = 80$ Hz, $m = 30$ mg, and $Q = 68$ gives a thermal noise of 7 ng/rt Hz. In order to resolve the thermal noise, the proof mass displacement resulting from an acceleration of this value must be greater than the noise of the interdigital position sensor. Given that the displacement of a proof mass is the quotient of the acceleration and the square of its angular resonant frequency, the thermal displacement noise of the 80 Hz sensor is 3×10^{-3} Å/rt Hz. The noise of the interdigital position sensor is most likely dominated by wavelength fluctuations of the laser and has been previously found to have a $1/f$ characteristic and is approximately 10^{-3} Å/rt Hz at 40 Hz [10]. This noise is typically an order of magnitude greater than the photodetector shot noise. Since the position noise of the 80 Hz accelerometer is less than thermal displacement noise, we expect that the resolution should be primarily limited by the thermal noise under ideal conditions.

In order to compare the resolution of the 80 Hz device with its thermal noise, we measured its power spectrum density. The voltage noise was converted to a noise equivalent acceleration (NEA) by dividing the spectrum by the fitted sensitivity function. However, even with mechanical isolation, the background seismic noise of 0.1 to 10 μg is significantly greater than the thermal noise. To determine an upper limit of the NEA, we measured the coherence between the noise of two identical accelerometers. The coherence of two 80 Hz sensors is shown in Fig. 5. The upper limit of the NEA is found by scaling the noise of one of the devices by the root of the deviation of the coherence from unity as described by Barzilai *et al.* [2]. Fig. 6 shows

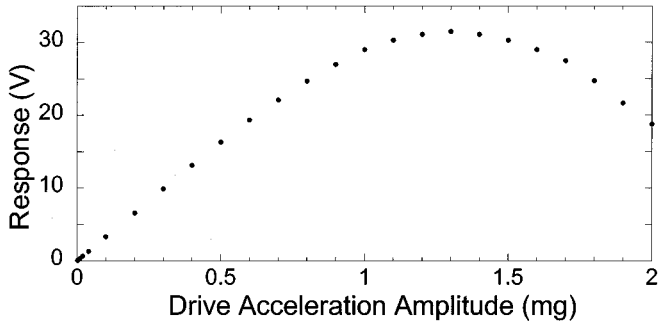

Fig. 7. Response from an 80 Hz resonant accelerometer that is drive with a 40 Hz sine wave of varying amplitude. The output is linear to 0.7 mg which corresponds to a dynamic range of 85 dB.

the initial NEA (seismic), scaled NEA (sensor) and the thermal noise given by (2). The scaled NEA is 40 ng/rt Hz at 40 Hz which is six times larger than thermal noise of 7 ng/rt Hz.

The linear range of the accelerometer was measured by varying the amplitude of a sine wave drive to the shaker. Fig. 7 shows the output linearity of the accelerometer when driven at 40 Hz. The open-loop dynamic range, or the ratio of the linear range to the resolution, is about 85 dB at 40 Hz. Recall that the intensity of each diffraction mode is a sine squared function of the finger offset. At large drive accelerations, the response no longer resembles the sine wave drive signal because of this nonlinear relationship. The linear acceleration range of 1 mg corresponds to a deflection range of 39 nm. The linear range (and sensitivity) can be maximized by adjusting the tilt of the accelerometer to set the static finger offset at a point of inflection in (1). In this case, the interferometric sensor would be linear to about a tenth of the wavelength of the light source, or 67 nm.

V. Conclusion

We have demonstrated that the interdigital position detector can be used to construct an accelerometer with a resolution of 40 ng/rt Hz at 40 Hz and a package volume of less than 9 cm^3. Furthermore, proof masses with resonant frequencies down to 80 Hz can be bulk-micromachined using a two mask, one wafer, CMOS-compatible process. The package volume can be further reduced by using a vertical cavity surface emitting laser (VSCEL) fabricated into a smaller photodiode die. A fabrication process that aligns and bonds an entire wafer of such dies to the proof mass wafer could reduce the cost and time to assemble the package. In this scenario, the packaging would only involve making electrical connections and protecting the sensor from the environment. Finally, the utility of the interferometric accelerometer can be increased (at the expense of simplicity) by adding force feedback to control the zero-input bias and sensitivity independent of the sensor's tilt.

The existing application of the interferometric accelerometer would be to quantify seismic disturbances, a measurement useful for vibration sensitive experiments. Other applications would be in triangulation, or the use of a network of accelerometers to localized low frequency disturbances such as a finger tap on a board or a person moving in a room.

Acknowledgment

The fabrication of the interferometric accelerometer was built on lessons learned in a laboratory course co-taught by Prof. Manalis and Prof. Schmidt. The class members, J. Hui, O. Nielsen, O. Olubuyide, C. Ryan, and J. Scholvin, investigated the application of a buried oxide layer to the original process and a novel method for device packaging. The authors would especially like to thank J. Scholvin for transferring his processing experience from the class. The fabrication was performed at the MIT Microsystems Technology Laboratories and aided by its staff and students, especially V. Diadiuk, B. Teynor, T. Takacs, D. Ward, K. Broderick, A. Fan, and I. Lauer. E. Cooper, P. Russo, and Prof. S. Seung contributed invaluably to the noise analysis.

References

[1] M. Stephens, "A sensitive interferometric accelerometer," *Rev. Sci. Instrum.*, vol. 64, no. 99, pp. 2612–2614, 1993.
[2] A. Barzilai, T. VanZandt, and T. Kenny, "Technique for measurement for the noise of a sensor in the presence of large background signals," *Rev. Sci. Instrum.*, vol. 69, no. 7, pp. 2767–2772, 1998.
[3] H. K. Rockstad, T. K. Tang, J. K. Reynolds, T. W. Kenny, W. J. Kaiser, and T. B. Gabrielson, "A miniature, high-sensitivity, electron tunneling accelerometer," *Sens. Actuators A*, vol. 53, pp. 227–231, 1996.
[4] C. H. Liu *et al.*, "Characterization of a high-sensitivity micromachined tunneling accelerometer with micro-g resolution," *J. Microelectromech. Syst.*, vol. 7, no. 2, pp. 235–243, 1998.
[5] T. Strobelt *et al.*, "Electron tunneling accelerometers for high resolution," in *Proc. 10th Int. Conf. Solid-State Sensors and Actuators*, 1999, pp. 1534–1537.
[6] C. H. Liu, A. Barzilai, O. Ajakaiye, H. K. Rockstad, and T. W. Kenny, "Performance enhancements for the micromachined tunneling accelerometer," in *Proc. 10th Int. Conf. Solid-State Sensors and Actuators*, 1999, pp. 1290–1293.
[7] D. Rugar, H. J. Mamin, and P. Guethner, "Improved fiber-optic interferometric for atomic force microscopy," *Appl. Phys. Lett.*, vol. 55, no. 25, pp. 2588–2590, 1989.
[8] S. R. Manalis, S. C. Minne, A. Atalar, and C. F. Quate, "Interdigital cantilevers for atomic force microscopy," *Appl. Phys. Lett.*, vol. 69, no. 25, pp. 3944–3946, 1996.
[9] G. G. Yaralioglu, A. Atalar, S. R. Manalis, and C. F. Quate, "Analysis and design of an interdigital cantilever as a displacement sensor," *J. Appl. Phys.*, vol. 83, no. 12, pp. 7405–7414, 1998.
[10] S. C. Minne, S. R. Manalis, and C. F. Quate, *Bringing Scanning Probe Microscopy up to Speed*. Boston, MA: Kluwer, 1999.
[11] N. C. Loh, "High-resolution micromachined interferometric accelerometer," Master's thesis, Massachusetts Institute of Technology, Cambridge, 2001.
[12] E. B. Cooper *et al.*, "High-resolution micromachined interferometric accelerometer," *Appl. Phys. Lett.*, vol. 76, no. 22, pp. 3316–3318, 2000.
[13] M. J. Novac, "Design and fabrication of a thin film micromachined accelerometer," Master's thesis, Massachusetts Institute of Technology, Cambridge, 1992.
[14] T. B. Gabrielson, "Mechanical-thermal noise in micromachined acoustic and vibration sensors," *IEEE Trans. Electron Devices*, vol. 40, pp. 903–909, May 1993.

Nin C. Loh received the B.A. degree in physics from Pomona College, Claremont, CA, in 1999 and the M.S. degree in mechanical engineering from the Massachusetts Institute of Technology (MIT), Cambridge, in 2001.

He is currently a MEMS Engineer at Zyomyx, Inc., Hayward, CA.

Martin A. Schmidt (S'88–M'85–SM'00) received the B.S. degree in electrical and computer engineering from Rensselaer Polytechnic Institute, Troy, NY, in 1981 and the S.M. and Ph.D. degrees in electrical engineering and computer science from the Massachusetts Institute of Technology (MIT), Cambridge, in 1983 and 1988, respectively. His Ph.D. research concerned microsensors for measurement of turbulent boundary layers.

In 1988, he joined the faculty of the Electrical Engineering and Computer Science Department, MIT, where he is currently a Professor of electrical engineering. He is also the Director of the Microsystems Technology Laboratories, MIT. His research interests are in microfabrication technologies for realization of micromechanical and biological reactors, micromachined turbine engines, and microactuators. He has served on the program committees for many of the major meetings in the microelectromechanical systems (MEMS) field and currently serves on the International Steering Committee for Solid-State Sensors and Actuators.

Dr. Schmidt was the recipient of the National Science Foundation Presidential Young Investigator Award and the Ruth and Joel Spira Teaching Award presented by MIT.

Scott R. Manalis received the B.S. degree in physics from the University of California, Santa Barbara, in 1994 and the Ph.D. degree in applied physics from Stanford University, Stanford, CA, in 1998.

Currently, he is an Assistant Professor of Media Arts & Sciences and Bioengineering at the Massachusetts Institute of Technology (MIT), Cambridge. His research interests are on the development of nanofabrication technologies for building molecular-scale devices, the use of MEMS for novel detection schemes, and the application of such devices to biology.